BJRS
BRAZILIAN JOURNAL OF RADIATION SCIENCES

org/10.15392/2319-0612.2025.2868
Braz. J. Radiat. Sci., Rio de Janeiro
2025, 13(4) | 01-23 | e2868
Editor: Prof. Dr. Bernardo Maranhão Dantas
Editor: Prof. Dr. Alfredo Lopes Ferreira Filho
Submitted: 2025-02-26
Accepted: 2025-10-30

Computational Analysis of Gamma-Ray and Fast Neutron Attenuation performance of some Thorium and Uranium Compounds

Osman, A. M.*

Department of Physics, College of Science, Jouf University, P.O.Box 2014, Kingdom of Saudi Arabia

*Correspondence: amoa@ju.edu.sa

Abstract: Evaluation of the radiation shielding effectiveness of some compounds including Fe, Th, Y, Nb, Ta, Ti, and U have been computed for energy absorption and total interaction in the photon energy range from 0.015 to 15 MeV. The effective atomic number (Z_{eff}), of these compounds was determined via the mass attenuation (μ/ϱ, cm^2/g) and mass energy absorption (μ/ϱ, cm^2/g)en coefficients. Accordingly, the values of Z_{eff} have been computed for total photon interaction (Z_{Ieff}) and energy absorption (Z_{Aeff}) using Py-MLBUF and Phy-X/PSD codes. The effective removal cross section for fast neutrons (Σ_R, cm^{-1}) and attenuation lengths were also calculated to study the attenuation properties of fast neutrons. The results displayed showed that, Z_{eff} of S1 (UO2) and S2 (ThSiO4) are comparatively higher than the Zeff of the remaining compounds, while S7 (Fe(UO2)2(PO4)2.8(H2O)) possesses the lowest values of Z_{eff}. The obtained results also show that Z_{Aeff} should be used instead of Z_{Ieff} when the quantity of interest is energy dissipation. In addition, the calculated values of Σ_R for the tested compounds were found to be close and ranged from 0.079 cm^{-1} for S4 to 0.146 cm^{-1} for S1. Moreover, comparison of the calculated values for different shielding parameters showed good agreement between the proposed methods. Finally, this study could be useful in applications of these compounds for shielding requirements from gamma-ray and fast neutron in different fields such as, nuclear fuel cycles and medical shielding in uranium-handling environments.

Keywords: Shielding effectiveness, Energy absorption, Effective atomic number, effective removal cross-section.

BJRS
BRAZILIAN JOURNAL OF RADIATION SCIENCES

doi.org/10.15392/2319-0612.2025.2868
Braz. J. Radiat. Sci., Rio de Janeiro
2025, 13(4) | 01-23 | e2868
Editor: Prof. Dr. Bernardo Maranhão Dantas
Editor: Prof. Dr. Alfredo Lopes Ferreira Filho
Submitted: 2025-02-26
Accepted: 2025-10-30

Análise computacional do desempenho de atenuação de raios gama e neutrões rápidos de alguns compostos de tório e urânio

Resumo: A avaliação da eficácia da proteção contra a radiação de alguns compostos, incluindo Fe, Th, Y, Nb, Ta, Ti e U, foi calculada para a absorção de energia e interação total na gama de energia dos fotões de 0,015 a 15 MeV. O número atómico efetivo (Z_{eff}) destes compostos foi determinado através dos coeficientes de atenuação de massa (μ/ρ, cm^2/g) e de absorção de energia de massa (μ/ρ, cm^2/g). Por conseguinte, os valores de Z_{eff} foram calculados para a interação total dos fotões (Z_{Ieff}) e a absorção de energia (Z_{Aeff}) utilizando os códigos Py-MLBUF e Phy-X/PSD. Além disso, a secção transversal de remoção efectiva para neutrões rápidos (ΣR, cm^{-1}) e os comprimentos de atenuação foram calculados para investigar as caraterísticas de atenuação de neutrões rápidos. Os resultados apresentados mostraram que, Z_{eff} de S1 (UO_2) e S2 ($ThSiO_4$) são comparativamente mais elevados do que os Z_{eff} dos restantes compostos, enquanto S7 ($Fe(UO_2)_2(PO_4)_{2.8}(H_2O)$) possui os valores mais baixos de Z_{eff}. Os resultados obtidos também mostram que Z_{Aeff} deve ser usado em vez de Z_{Ieff} quando a quantidade em questão é a dissipação de energia. Além disso, os valores calculados de Σ_R para os compostos testados foram encontrados próximos e variaram de 0,079 cm^{-1} para S4 a 0,146 cm^{-1} para S1. Além disso, a comparação dos valores calculados para diferentes parâmetros de proteção revelou uma boa concordância entre os métodos propostos. Por último, este estudo poderá ser útil para aplicações destes compostos em requisitos de proteção contra raios gama e neutrões rápidos em diferentes domínios, tais como os ciclos do combustível nuclear e a proteção médica em ambientes de manuseamento de urânio.

Palavras-chave: Eficácia da blindagem, Absorção de energia, Número atómico efetivo, Secção transversal de remoção efectiva.

1. INTRODUCTION

Recently, nuclear technology is often used on a large scale such as materials identification, agriculture, medical applications, nuclear power plants, scientific and space exploration. A lot of literature focuses on investigated a new shielding material to control the external exposure doses. In general, γ-photon attenuation coefficients described the radiation interaction with matter. For interaction of γ-photon with compound/composite materials in which the number of elements is in varying proportions, one should especially note the effective atomic number (Z_{eff}). This is the main important feature among the photon interaction coefficients which is used in evaluating different quantities for shield design. This quantity is introduced to express the properties of composite materials in terms of equivalent elements [1]. Literatures and studies on Z_{eff} for total photon interaction were performed for several materials including building materials [2], glass systems [3-5], compounds [6-8], alloys [9-11], biological materials [12, 13], hydride and borohydride metals [14].

However, evaluation Z_{eff} in composite materials for both photon energy absorption and photon interaction in continuous energy range appears to be rare [15–19]. To design an effective shield, apart from X-rays, gamma rays and neutrons are the main types of radiation, which must be considered. Estimation of the fast neutrons attenuation through the shielding materials can be evaluated by computing fast neutron removal cross-sections (Σ_R, cm^{-1}) [20]. A few literatures deal with the evaluation of fast neutron attenuation in different media [21, 22].

The aim of the present work is to evaluate the shielding behavior of some nuclear oxides materials of thorium, uranium and the host rocks themselves. These compounds have garnered significant interest due to their potential applications in the nuclear industry, luminescence, ionic conductivity, and nuclear waste immobilization. The use of these materials as radiation shields offers a promising solution to some problems in the nuclear

industry. The shielding capabilities of the proposed compounds were computed by analyzing various shielding parameters as follows: (a) evaluation of γ-photons interaction and photon energy absorption parameters in terms of effective atomic number in the energy range from 15 keV to 15 MeV, (b) comparison of the proposed methods used for computation of Z_{1eff} and Z_{Aeff} and (c) Z_{eff} were computed for some well-known γ-ray sources; ^{22}Na, ^{55}Fe, ^{60}Co, ^{109}Cd, ^{131}I, ^{133}Ba, ^{137}Cs, ^{152}Eu, and ^{241}Am, (d) investigate the fast neutron attenuation characteristics in terms of Σ_R, and attenuation length for incident neutrons with energy of 4 MeV.

2. MATERIALS AND METHODS

This work is devoted to investigate the shielding performance of some U and Th compounds using Py-MLBUF [23] and Phy-X/PSD [24] codes. The Phy-X/PSD software is available at https://phy-x.net/PSD, and has been developed for calculation of different parameters for radiation shielding and dosimetry. On the other hand, Py-MLBUF is a computer code has been written for computation of various gamma-ray shielding parameters and is available at https://pymlbuf.pythonanywhere.com. The elemental constituent and physical properties of the investigated materials are shown in table 1. Methods for computing of various shielding parameters are given and discussed in the following section.

Table 1 : Physical properties and chemical formula for the examined compounds

Sample	Code	Chemical formula	Density (g/cm³)	Electron Density (g/cm³)	Molar mass (g/mol)
Uranium dioxide	S1	UO2	10.97	8.78	270.028
Huttonite	S2	ThSiO4	7.1	5.96	97.064
Pyrochlore	S3	(Na,Ca)2Nb2O6(OH.F)	5.3	4.93	353.84
Euxenite-(Y)	S4	(YCaCe)(NbTaTi)2O6	4.84	4.35	392.28
Metauranocircite	S5	Ba(UO2)2(PO4)2.6-8(H2O)	3.95	3.47	993.43
Allanite-(Y)	S6	(YCeCa)2(AlFe)3(SiO4)3(OH)	3.75	3.55	598.63
Bassetite	S7	Fe(UO2)2(PO4)2.8(H2O)	3.63	3.31	

3. THEORETICAL BACKGROUND

In this study, the parameters of photon interaction and energy absorption in a wide energy range (0.015 to 15 MeV) were presented and discussed. These investigation includes different parameters such as mass attenuation (μ/ϱ, cm^2/g), mass energy absorption $(\mu/\varrho, cm^2/g)_{en}$ coefficients and effective atomic number Z_{eff}. The calculation procedure for obtaining the effective atomic number by the direct method is described by [18]. The direct method for calculating the effective atomic number Z_{eff} of a compound/mixture is derived from the total mass attenuation coefficient $\left(\frac{\mu}{\rho}\right)_T$. This coefficient can be estimated by:

$$\left(\frac{\mu}{\rho}\right)_T = \sum f_i \left(\frac{\mu}{\rho}\right)_i \qquad (1)$$

The cross section per molecule (σ_m) can be calculated using the following equation:

$$\sigma_m = n\sigma_a = nZ_{eff}\sigma_e \qquad (2)$$

Where $n = \Sigma_i n_i$, which expresses the total number of atoms in the molecule.

Then, σ_m can be written as:

$$\sigma_m = \sum_i n_i \sigma_i \qquad (3)$$

Where σ_i and n_i are the atomic cross section and the number of atoms of the i^{th} element of the molecule. From Equs. (1) and (2) one can be obtained:

$$\sigma_a = \frac{\sigma_m}{n} = \frac{\Sigma_i n_i \sigma_i}{n} \qquad (4)$$

$$\sigma_e = \frac{\sigma_m}{nZ_{eff}} = \frac{1}{n}\sum_i n_i \frac{\sigma_i}{Z_i} \qquad (5)$$

Where Zi is the atomic number of the i^{th} element. Thus, the effective atomic numbers of the sample can be given by:

$$Z_{I_{eff}} = \frac{\sigma_a}{\sigma_e} = \frac{\sum_i f_i A_i (\frac{\mu}{\rho})_i}{\sum_i f_i \frac{A_i}{Z_i} (\frac{\mu}{\rho})_i} \qquad (6)$$

Where $Z_{I_{eff}}$, A_i, f_i and $(\frac{\mu}{\rho})_i$ are the effective atomic number for photon interaction, atomic mass, mole fraction and mass attenuation coefficient respectively.

The effective atomic number for photon energy absorption $Z_{A_{eff}}$ can be estimated using Equ. **(6)** by replacing the mass attenuation coefficient with the mass energy absorption coefficient $(\mu/\rho)_A$. The $(\mu/\rho)_A$ values have been obtained from the tabulated data [25].

For the given materials, Py-MLBUF platform was used to compute the effective atomic number for photon interaction and absorption ($Z_{I_{eff}}$ and $Z_{A_{eff}}$) respectively. For a comparison the effective atomic number was computed using Phy-X/PSD software.

On the other hand, the attenuation of fast neutrons is given in term of the effective removal cross-section, $\sum_R$ (cm^{-1}). For the investigated compounds, the values of Σ_R can be computed by Phy-X/PSD code and the results were validated using the following relation [**26**]:

$$\Sigma_R = \sum_i W_i (\Sigma_R/\rho)_i \qquad (7)$$

Where, W_i and $(\sum_R/\varrho)_i$ are weight fraction and the mass removal cross section of the i^{th} constituent element.

4. RESULTS AND DISCUSSIONS

4.1. Mass attenuation coefficient (μ_m)

The mass attenuation coefficient (μ_m) is the main quantity that describes the absorption properties of materials. For better materials to protect against gamma radiation, μ_m should be higher [23]. Computed results for the total photon interaction (μ/ϱ) as a

function of photon energy for the tested samples are shown in Figure 1. It can be seen from the displayed figure that the total (μ/ϱ) values are very high in the region with low photon-energy. Then the obtained values gradually decrease and become their lowest levels in the medium energy region. In the high energy-region the displayed values begin to increase. Another important quantity is $(\mu/\varrho)_A$, which expresses the mass energy absorption coefficient. This parameter is a good approximation of the amount of photon energy available to produce the chemical, biological and other effects associated with exposure to ionizing radiation and is therefore useful for calculating absorbed dose in different fields. Figure 2 displayed the calculated results of $(\mu/\varrho)_A$ for the investigated samples as a function of photon energy. The displayed figure showed that $(\mu/\varrho)_A$ gives almost the same behavior as the total mass attenuation coefficient (μ/ϱ). This figure also indicated that the calculated values of $(\mu/\varrho)_A$ are generally lower than the corresponding values of $(\mu/\varrho)_I$.

Figure 3 shows the variations of attenuation coefficient for total and partial photon interactions in UO_2 sample. It can be seen from this figure that different interactions are dominant at different energy ranges. In the very low photon energy range, photoelectric absorption dominates over both coherent and incoherent scattering (Compton Effect) in the given energy range. After that, the Compton Effect becomes the dominant interaction until the end of the range. It is also noted that pair production in the nuclear field begins when the photon energy is higher than $2m_ec^2$ (1.02 MeV), and the probability increases with increasing the photon energy, until it reaches a plateau at high energy. If the photon energy is more than $4m_ec^2$ (2.044 MeV), the reaction can also occur in the atomic electron field (pair production in the electron field). As well as, this figure indicated that, the Compton scattering curve is bifurcated because it depends on the probability of photon interaction with incoherent scattering for the corresponding energy. Finally, this figure presented the variation of mass energy absorption coefficient ($(\frac{\mu}{\rho})_A$, cm^2/g) which is based only on the energy absorbed into the medium. Therefore, energy losses due to Compton scattering,

bremsstrahlung, and other radiative processes following interaction have been subtracted because they are very likely to leave the medium. This justifies the lower values of $(\frac{\mu}{\rho})_A$ in general than the values of $\left(\frac{\mu}{\rho}\right)_{total}$ as shown in Figure 3. The $(\frac{\mu}{\rho})_A$ is the most important parameter for determining radiation dose when the photon flux can be determined [27].

Figure 1: Variations of $(\mu/\varrho)_I$ for the investigated samples against photon energy

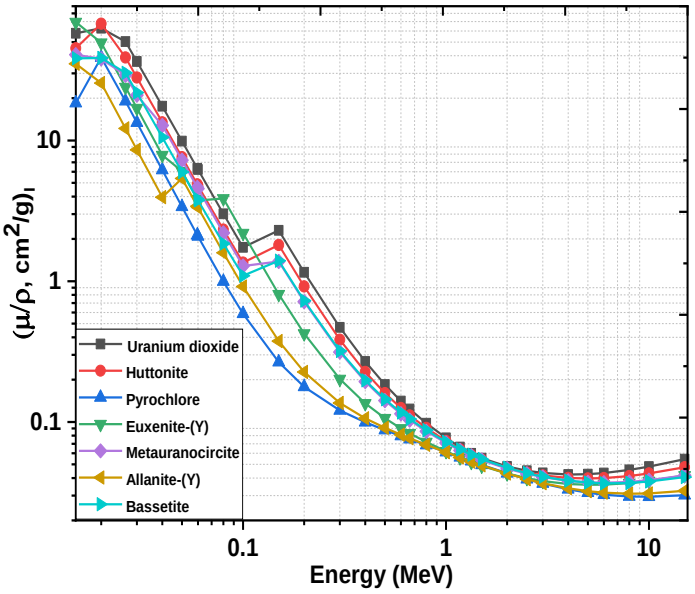

Figure 2: Variations of $(\mu/\varrho)_A$ for the investigated samples against photon energy.

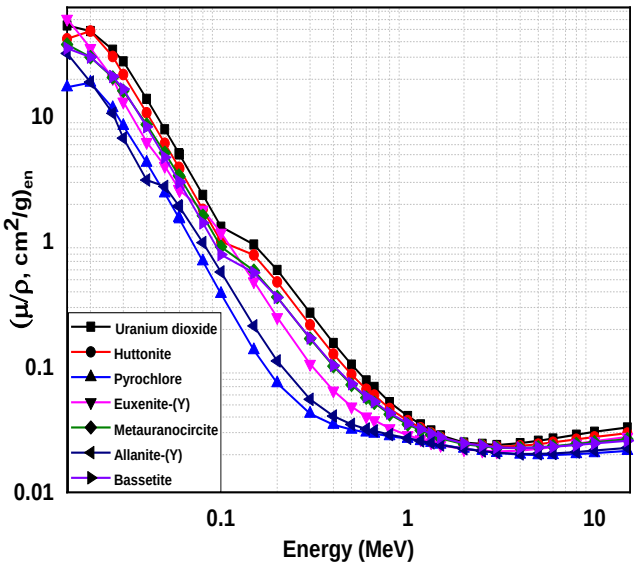

Figure 3: Variation of $\left(\frac{\mu}{\rho}\right)_{total}$ values for UO_2 sample against photon energy

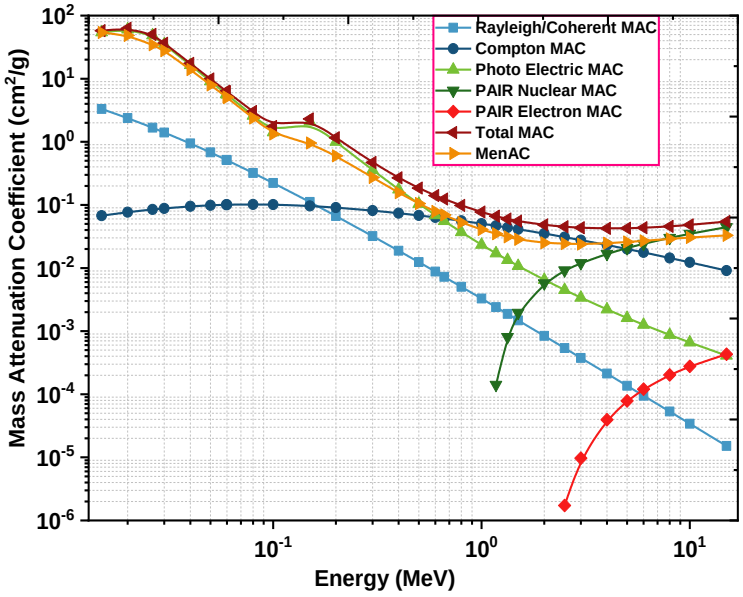

4.2. Effective atomic number (Z_{eff})

The total cross-section areas that an atom and an electron of a material offer for photons attenuation and energy absorption are given in the term (σ_a and $\sigma_{a(en)}$, cm^2), and (σ_{el} and $\sigma_{el(en)}$, cm^2), respectively. These quantities give the precise probability of radiation interactions per atom or electron in each unit volume of shielding material [28]. Higher values of σ_a and σ_{el} result in better shielding due to the increased probability of collision between photons and atoms, resulting from the higher cross-sections. Figures 4(a - d) exhibit their variation with energy. It can be observed from these figures that σ_a and σ_e follow a similar trend with energy, both decreasing with the rise in energy. In general, the values of σ_a are larger than their corresponding σ_{el} in both photons attenuation and energy absorption. One noticeable difference between σ_a and σ_{el} is observed in the energy range 0.5 – 4 MeV, where these quantities vary within samples. Finally, the displayed figures showed that both σ_{el} and σ_a are higher for S1 sample over the selected energy range (0.015 – 15 MeV).

Figure 4: Behaviors of (a) Atomic Interaction Cross section for Attenuation, (b) Electron Interaction Cross section for Attenuation, (c) Atomic Interaction Cross section for Absorption, and (d) Electron Interaction Cross section for Absorption

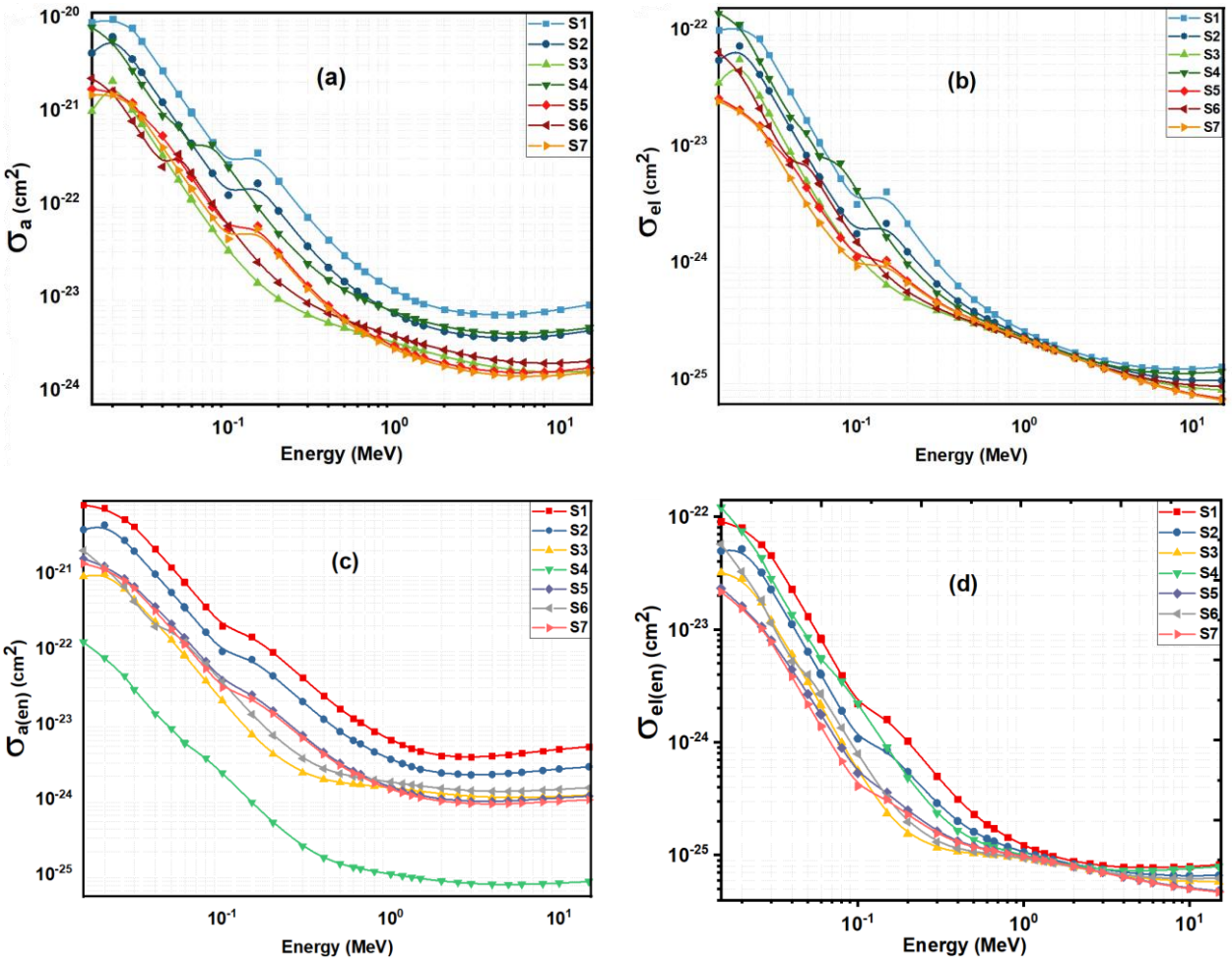

The effective atomic number (Z_{eff}) is an imperative quantity that describes the attenuation capability of the composite materials. This quantity is given by the actual amount of positive charge experienced by an electron in a multi-electron atom. Z_{eff} can be evaluated using the relation: $Z_{eff} = \sigma_a \sigma_{el}^{-1}$ [28]. High values of Z_{eff} are preferred because there will be a higher chance of photon collision with substances [29]. This parameter cannot be expressed in a one number because different interaction processes contribute as a function of photon energy and the atomic numbers present in the compound must be weighted differently [30]. Calculations of Z_{eff} in terms of photon interaction (Z_{Ieff}) and photon energy absorption (Z_{Aeff}) for the investigated compounds were performed using Py-MLBUF and Phy-X/PSD codes.

The variation of Z_{Ieff} and Z_{Aeff} as a function of photon energy for the investigated compounds are presented in Figures 5 - 9. Hence, it is known that the effective atomic number is an energy-dependent parameter. These figures indicated that, at low-energy range (0.015 - 0.05 MeV), the maximum value of Z_{eff} was found. In this range, the total atomic cross section and hence Z_{eff} are proportional to Z^{4-5}, where the photoelectric absorption is the main predominant process. At the energy range 0.05 - 5 MeV, where the main interaction is the Compton scattering, Z_{eff} is proportional to Z. At this region the obtained values become nearly constant. At high energies (> 5 MeV), Z_{eff} is proportional with Z^2 where the pair production is the main interaction. Therefore, these figures show observed peaks in the very low energy region. These peaks are due to the K-absorption edge of heavy elements present in the examined compounds such as U, Th, Nb, and Ce. As well as, the computed values of Z_{Ieff} and Z_{Aeff} increase again with increasing the photon energy. Moreover, the displayed figures indicated that there is no energy region clearly dominated by Compton scattering. This can be attributed because Compton scattering is dominant for low and medium Z elements. In addition to the corresponding energy values at which the maximum Z_{Aeff} and Z_{Ieff} occur, they also differ for the tested samples. These results also indicated that the width of the transition energy depends on the photon energy in the region of photoelectric absorption and Compton scattering. The transition energy from photoelectric absorption to Compton scattering results in higher energies for absorption (2 MeV) when compared to interaction process (~1.5 MeV). These phenomena can be explained by the fact that photoelectric absorption is the main dominant for the examined samples at low energy region. Therefore, it can be concluded that photoelectric effect is more important than Compton scattering for the absorption process. The computed values of Z_{Aeff} and Z_{Ieff} for UO_2 sample for some common gamma ray sources are given in table 2. The tabulated data reflects that the value of Z_{Aeff} is generally larger than the corresponding value of Z_{Ieff} at a given photon energy.

Table 2 : Computed values of Z_{Aeff} and Z_{Ieff} for UO2 sample

Source	Energy (MeV)	Z_{Ieff}	Z_{Aeff}
$^{241}_{95}Am$	0.02634	90.9334	90.9625
	0.05954	88.6608	91.2789
$^{137}_{59}Cs$	0.662	51.7669	60.3082
$^{60}_{27}Co$	1.173	43.7643	46.8651
	1.330	42.8839	44.9338

To compare the proposed methods, the computed results of relative differences (RD) for the examined compounds are shown in Figures 5b), 6b), 7d), and 8c). By examining the data presented in these figures, it appears that the average RD ranges between 3.1 and 5.9%. In addition, the change in Z_{eff} behavior with the change in the weight fraction (%) of the heavy element in the compound was examined by evaluating RD_{max}. The calculated result for RD_{max} was plotted as a function of U weight fraction (%) and presented in Figure 7e. This figure clearly shows that the difference between Z_{Aeff} and Z_{Ieff} is inversely proportional with the weight fraction (%) of uranium-based compounds. Because of these significant differences between Z_{Aeff} and Z_{Ieff}, it is preferable to use Z_{Aeff} rather than Z_{Ieff} when examining the shielding performance of such materials with regard to energy deposition.

$$\boldsymbol{RD\ (\%) = \frac{(Z_{A_{eff}} - Z_{I_{eff}})}{Z_{A_{eff}}}\ x\ 100} \qquad \textbf{(8)}$$

Figure 9 displayed the computed Z_{eff} by using Phy-X/PSD code for the investigated compounds of some common γ-ray sources (^{22}Na, ^{55}Fe, ^{60}Co, ^{109}Cd, ^{131}I, ^{133}Ba, ^{137}Cs, ^{152}Eu and ^{241}Am). The displayed results indicated that Z_{eff} is an energy dependent quantity. Thus, it has higher value at lowest photon energy. The computed results show that Z_{eff} decreases rapidly in the low energy value (from 0.3 to 1.5 MeV) because the photoelectric effect is the main process in that range. Above 1.5 MeV of energy, the curve shows the desire in the value of Z_{eff} which reflects a good radiation shielding capability. The computed results also depend on the density of the sample. It can be seen from this figure that the values of sample S1

have the highest value compared to the other samples examined. These results also support the possibility of using the investigated samples to construct good shielding materials.

Figure 5: Variations of a) Z_{eff} for Allanite-(Y) compound against photon energy, b) Relative difference for Z_{eff} calculated by different methods

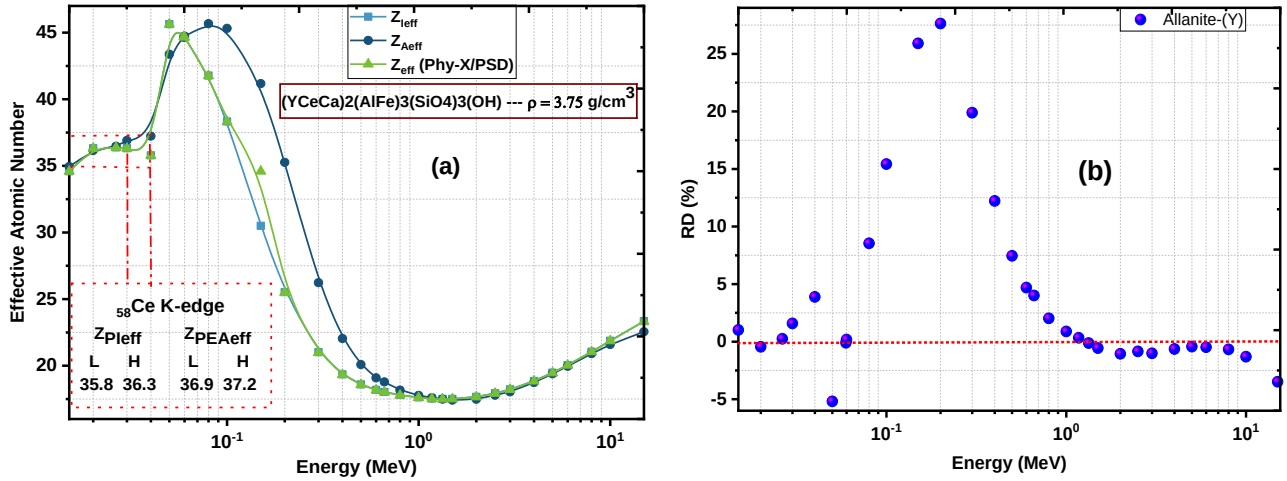

Figure 6: Variations of a) Z_{eff} for Huttonite compound against photon energy, b) Relative difference for Z_{eff} calculated by different methods.

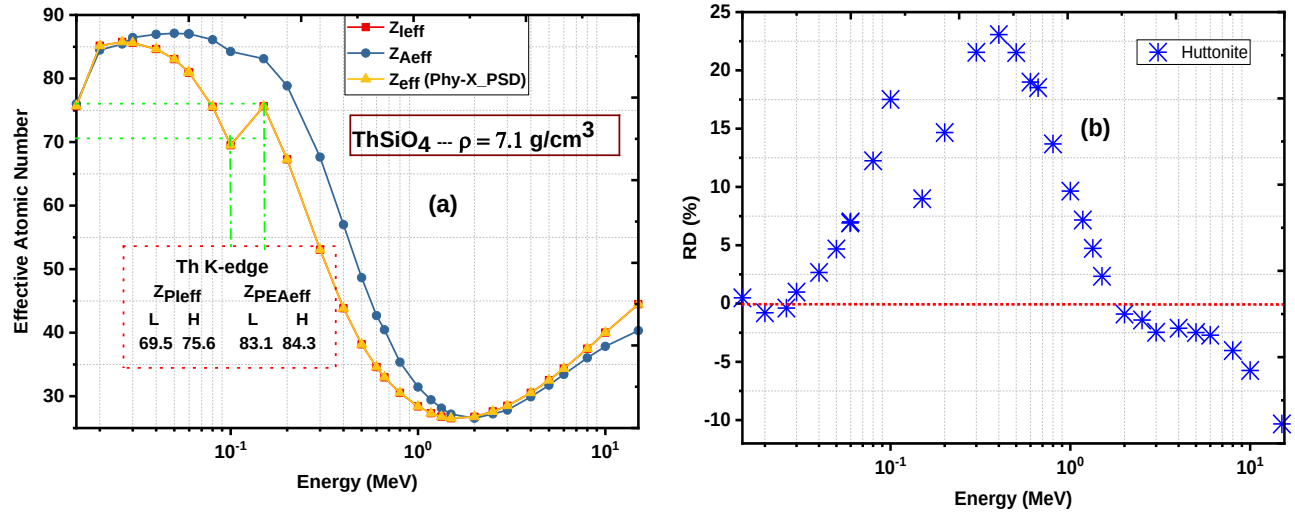

Figure 7: Variations of a-c) Z_{eff} for $^{238}_{92}U$ based compounds against photon energy, d) Relative difference for Z_{eff} calculated by different methods, and e) Maximum relative differences for Z_{eff}

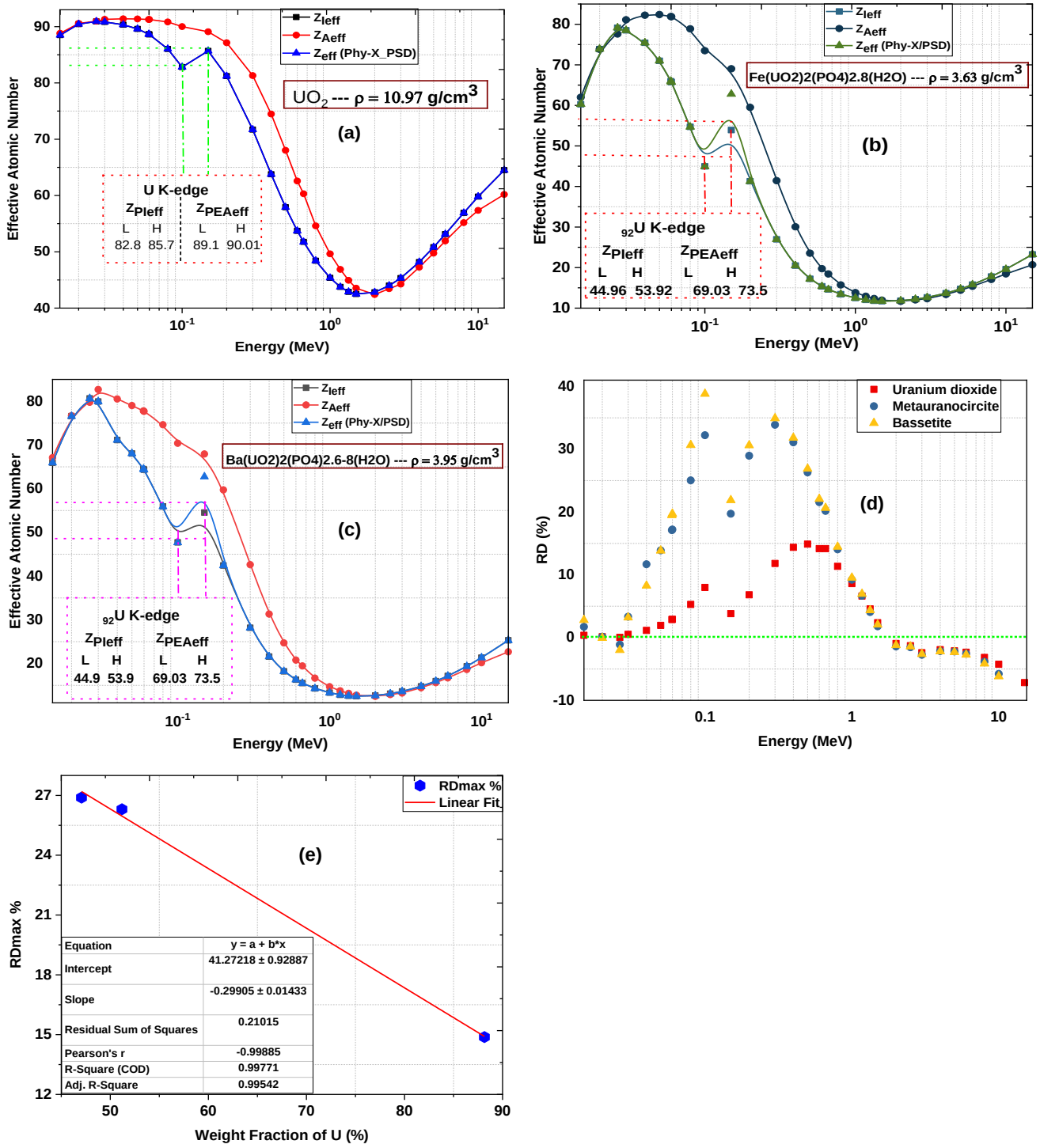

Figure 8: Variations of a-b) Z_{eff} for $^{237}_{93}Nb$ based compounds against photon energy, c) Relative difference for Z_{eff} calculated by different methods

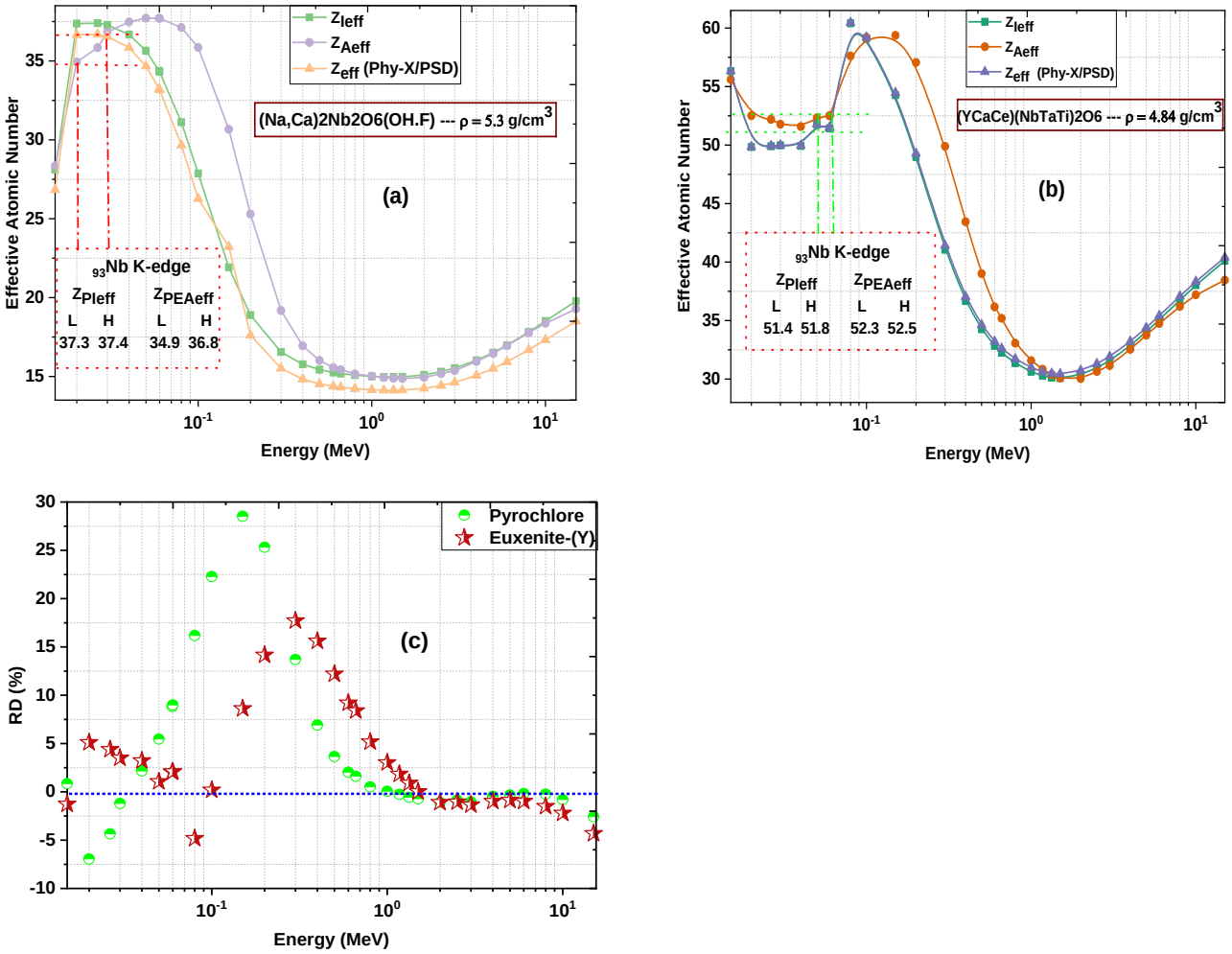

Figure 9: Variations of Z_{eff} of investigated compounds x photons energy emitted from some well-known γ-ray sources

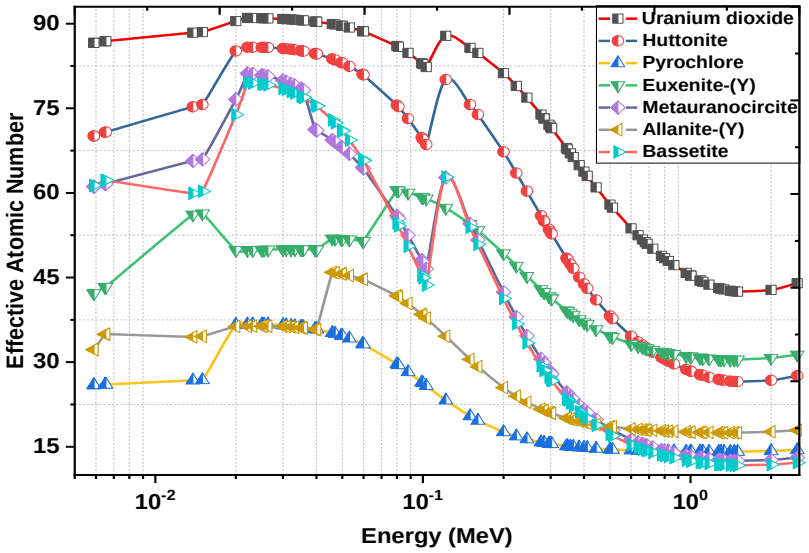

4.3. Fast neutron calculations

The attenuation of fast neutrons was evaluated by calculating the effective removal cross section (Σ_R, cm^{-1}). This parameter is the main quantity to measure the ability of the medium to remove fast/fission neutron from the incident beam. The values of Σ_R for the examined samples were computed by:

$$\Sigma_R = \sum_i \rho_i (\Sigma_R/\rho)_i \qquad (9)$$

Where, $(\Sigma_R/\varrho)_i$ and ϱ_i are respectively the mass removal cross-section and partial density of the i^{th} constituent.

For more evaluation, Σ_R in unit of cm^{-1} was computed using direct method by Equ. (9) and Phy-X/PSD code. Calculations were performed for the tested samples at neutron energies of 4 MeV. Σ_R of the selected samples is listed in table 3 and shown graphically in Figure 10.a. Samples S1 and S3 show a good fast neutron attenuation performance compare to the other examined compounds. Accordingly, S1 sample has the advantage of high attenuation for γ-photon and fast neutrons. In addition, the calculated results also showed a

difference between the values obtained using the proposed methods. Therefore, the relative deviation (δ) for the calculated results can be evaluated using the following relation:

$$\delta = \left| \frac{\sum_R D - \sum_R Phyx}{\sum_R D} \right| * 100 \qquad (10)$$

The relative deviation (δ %) values were listed in table **3** and displayed graphically in Figure 10.b. The calculated values of δ % reflect good agreement between the proposed methods, where δ % values varied from 0.03 % to 6 % for the tested compounds**.**

Table 3: The computed results of Σ_R (cm^{-1}) and relative deviation (δ %) for the proposed methods

Sample	Σ_R (cm^{-1})$_{Phy\text{-}X/PSD}$	Σ_R (cm^{-1})	Attenuation Length (cm)	δ %
S1	0.146	0.1465	6.826	0.036
S2	0.125	0.1247	8.019	0.031
S3	0.145	0.1454	6.878	0.031
S4	0.079	0.08157	12.259	3.194
S5	0.120	0.1287	7.770	6.704
S6	0.087	0.0894	11.186	3.064
S7	0.118	0.1177	8.496	0.053

Figures 10: a) Comparison of Σ_R (cm^{-1}) for investigated samples. b) The relative deviation (δ %) values

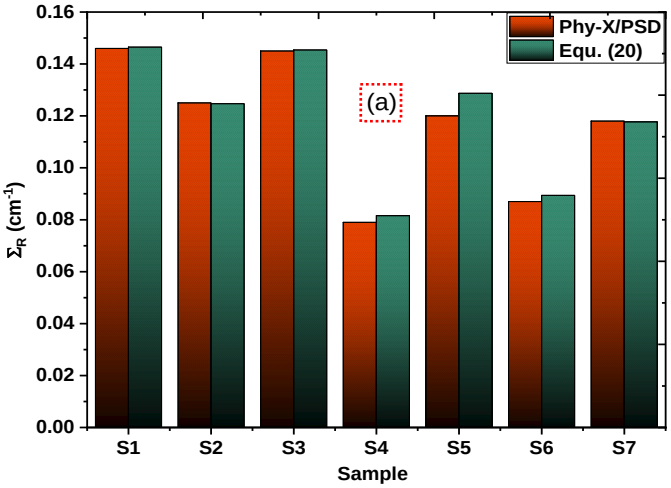

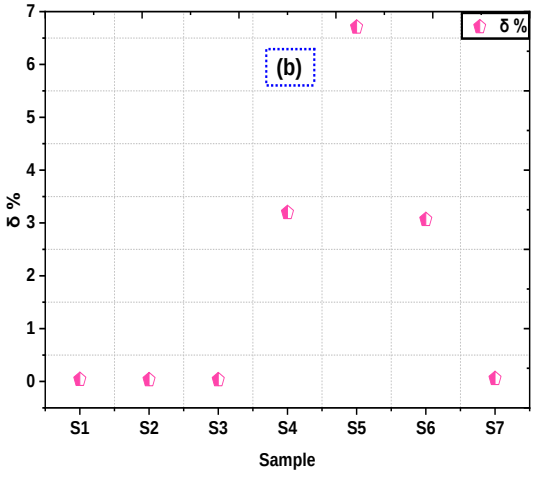

To study the effect of heavy metal concentration on the calculated values of Σ_R/ϱ, the variation of Σ_R/ϱ for uranium-based compounds x uranium weight (%) was displayed in Figure 11. As shown in this figure, the computed values of Σ_R/ϱ decrease with the increase of U weight (%) for the tested uranium-based compounds. Due to these noticeable variations, it should be reasonable to select the compounds with higher Σ_R/ϱ values when designing a shield for fast neutrons. Contributions of the constituent elements to Σ_R for the investigated compounds were displayed in Figures 12 (a-c). As shown from these figures, light and heavy elements contribution to Σ_R varies from one compound to another. This can be referred to the partial effective removal cross sections of the constituent elements. These figures also show that hydrogen has a significant contribution to Σ_R, although its weight (%) is very small in the tested compounds, 0.227039%, 1.594452%, 0.093333%, and 1.734155% for S3, S5, S6, and S7, respectively. This situation can be explained by the fact that elements with smaller atomic masses are more effective against fast neutrons.

Figure 11: Variation of Σ_R/ϱ with uranium weight (%) for uranium-based compounds

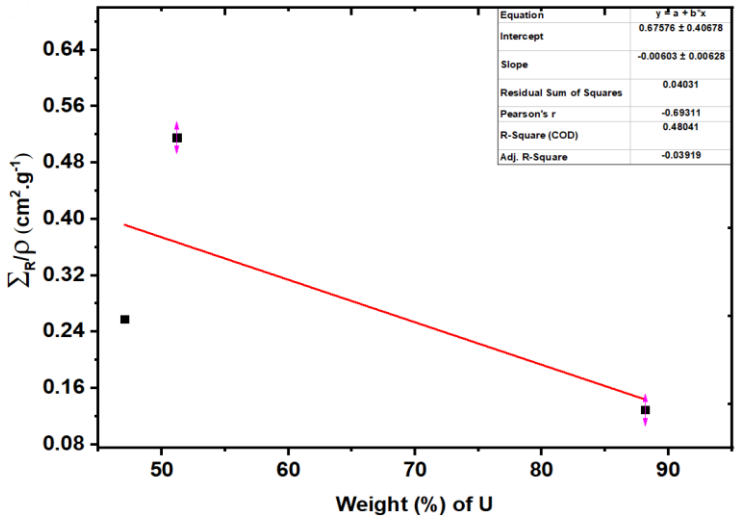

Figure 12: Contributions of the constituent elements to Σ_R for the investigated compounds

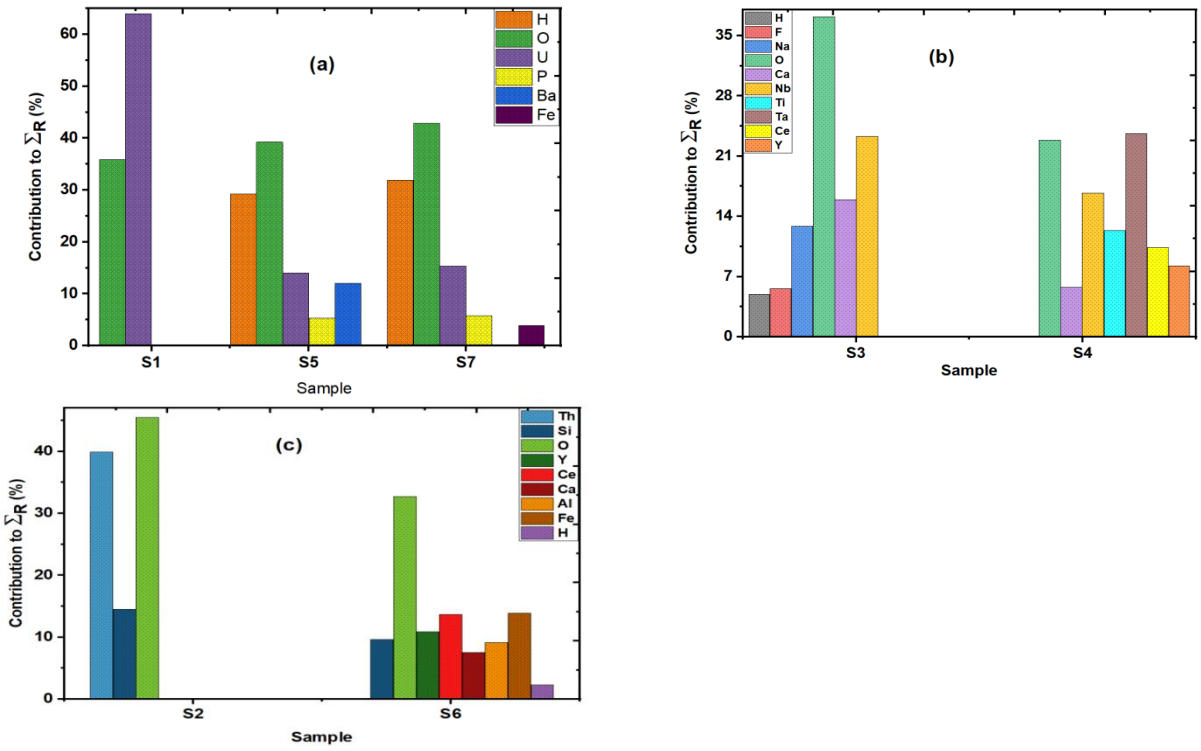

5. CONCLUSION:

The attenuation properties of γ-photons and fast neutrons for some U and Th compounds materials were evaluated through this study. The shielding effectiveness of the proposed materials was evaluated by using computer-based software Phy-X/PSD and Py-MLBUF for γ-photons in a wide energy range (0.015 to15 MeV). The neutron attenuation properties were investigated using the effective removal cross section (Σ_R) and attenuation length for fast neutrons parameters.

The obtained results indicate that samples coding S1 and S2 have the highest mass attenuation (μ/ϱ, cm^2/g) and mass energy absorption $(\mu/\varrho, cm^2/g)_{en}$ coefficients values while S7 sample has the lowest corresponding values. Then, S1 and S2 samples (the highest density samples ϱ = 10.97 g/cm^3 and 7.1 g/cm^3 respectively) are good absorber of γ-photons compared to other investigated compounds. As well as S1 and S2 samples have the highest

Z_{Aeff} and Z_{Ieff} values in contrast to other examined compounds. There are different observed breaks in the results obtained of Z_{Ieff} and Z_{Aeff}. These beaks are due to photoelectric effect near the K-absorption edge of the heavy constituent elements of the examined compounds. The best Z_{Ieff} and Z_{Aeff} values obtained for S1 and S2 samples reflect that γ-photons have a big chance of interacting. Moreover, the results obtained indicated significant variations between Z_{Aeff} and Z_{Ieff}. So, it is preferable to use Z_{Aeff} rather than Z_{Ieff} when evaluating the material shielding characteristics with respect to the energy deposition. The obtained Σ_R values for investigated samples vary from 0.146 to 0.079 cm^{-1}. So, samples coding S1 and S3 have higher values of Σ_R and lowest values of attenuation length, thus can be preferred as attenuator of fast neutrons. Therefore, it is clear that S1 sample has a good attenuation performance for both γ-ray and fast neutrons. Consequently, these samples can be proposed as a fast neutron/gamma-ray screen for different applications, such as the nuclear industry and medical protection in uranium handling environments.

FUNDING

No funding was received for this work

CONFLICT OF INTEREST

The author declares that he has no conflicts of interest.

REFERENCES

[1] Kaewkhao, J., et al., Determination of effective atomic numbers and effective electron densities for Cu/Zn alloy, **Journal of Quantitative Spectroscopy and Radiative Transfer**, v. 109, n. 7, p. 1260-1265, 2008, doi: https://doi.org/10.1016/j.jqsrt.2007.10.007.

[2] Kurudirek, M, et al., Chemical composition, effective atomic number and electron density study of trommel sieve waste (TSW), Portland cement, lime, pointing and their admixtures with TSW in different proportions. **Appl. Radiat. Isot.**, v. 68, n. 6, p. 1006-11, 2010.

[3] Kirdsiri, K., et al., Gamma-rays shielding properties of xPbO:(100−x)B2O3 glasses system at 662keV, **Annals of Nuclear Energy**, v. 36, n. 9, p. 1360-1365, 2009, doi: https://doi.org/10.1016/j.anucene.2009.06.019.

[4] Singh, K., et al., Gamma-ray attenuation coefficients in bismuth borate glasses. **Nucl. Instrum. Methods B**, v. 194, p. 1–6, 2002.

[5] Singh, S., et al., Barium borate-fly ash glasses: as radiation shielding materials. **Nucl. Instrum. Methods B**, v. 266, p. 140–146, 2008.

[6] Ozdemir, Y. and Kurudirek, M., A study of total mass attenuation coefficients, effective atomic numbers and electron densities for various organic and inorganic compounds at 59.54 keV. **Ann. Nucl. Energy**, v. 36, p. 1769–1773, 2009.

[7] Kurudirek, M. and Ozdemir, Y., Determination of effective atomic numbers in some compounds for photoelectric process at 59.54 keV by using different methods. **J. X-ray Sci. Technol**., v. 18, p. 183–191, 2010.

[8] Osman, A. M., Calculation of Gamma and Neutron Shielding Parameters for Reinforced Polymer Composites, **ASME. *ASME J of Nuclear Rad Sci.***; v. 9, n. 1, p. 1-9, 2023, doi: https://doi.org/10.1115/1.4054547.

[9] Murty, V. R. K., Effective atomic numbers for W/Cu alloy for total photon attenuation. **Radiat. Phys. Chem.**, v. 71, p. 667–669, 2004.

[10] El-Kateb, A. H., et al., Determination of atomic cross-sections and effective atomic numbers for some alloys. **Ann. Nucl. Energy**, v. 27, p. 1333–1343, 2000.

[11] A. M. Abdelmonem, et al., Computing the gamma-ray, charged particles and fast neutron-shielding performances of selected alloys, **Radiation Effects and Defects in Solids**, v. 179, n. 9-10, p. 1105-1131, 2024.

[12] Gowda, S., et al., Studies on effective atomic numbers and electron densities in amino acids and sugars in the energy range 30–1333 keV. **Nucl. Instrum. Methods B**, v. 239, p. 361–369, 2005.

[13] Manjunathaguru, V. and Umesh, T.K., Effective atomic numbers and electron densities of some biologically important compounds containing H, C, N and O in the energy range 145–1330 keV. J. **Phys. B: At. Mol. Opt. Phys.**, v. 39, p. 3969–3981, 2006.

[14] Osman, A. M., Analysis of radiation shielding effectiveness of hydride and borohydride metals for nuclear industry, **International Journal of Advanced Nuclear Reactor Design and Technology**, v. 5, *n.* 1, p. 30-43, 2023.

[15] Manjunathaguru, V. and Umesh, T. K., Total interaction cross sections and effective atomic numbers of some biologically important compounds containing H, C, N and O in the energy range 6.4–136 keV. **J. Phys. B: At. Mol. Opt. Phys.**, v. 40, p. 3707–3718, 2007.

[16] Manohara, S.R., et al., Studies on effective atomic number, electron density and kerma for some fatty acids and carbohydrates. **Phys. Med. Biol.**, v. 53, p. 377–386, 2008a.

[17] Manohara, S. R., et al., Photon interaction and energy absorption in glass: a transparent gamma ray shield. **J. Nucl. Mater.**, v. 393, p. 465–472, 2009.

[18] Manohara, S.R., et al., The effective atomic number revisited in the light of modern photon-interaction cross section databases. **Appl. Radiat. Isot.**, v. 68, p. 784–787, 2010.

[19] Kurudirek, M., et al., Effective atomic number study of various alloys for total photon interaction in the energy region of 1 keV to 100 GeV. **Nucl. Instrum. Methods A**, v. 613, p. 251–256, 2010b.

[20] El-Khayatt, A.M. and El-Sayed Abdo, A., MERCSF-N calculation program for fast neutron qremoval cross-sections in composite shields. **Ann. Nucl. Energy**, v. 36, p. 832–836, 2009.

[21] El-Khayatt, A.M., Radiation shielding of concretes containing different lime/ silica ratios. **Ann. Nucl. Energy**, v. 37, p. 7991–995, 2010a.

[22] El-Khayatt, A.M., Calculation of fast neutron removal cross-sections for some compounds and materials. **Ann. Nucl. Energy***,* v. 37, *n.* 2, p. 218–222*,* 2010b.

[23] Kulwinder Singh Mann and Sukhmanjit Singh Mann, Py-MLBUF: Development of an online-platform for gamma-ray shielding calculations and investigations, **Annals of Nuclear Energy**, v. 150, p. 1 – 22*,* 2021.

[24] Erdem Sakar, et al., Phy-X/PSD: development of user friendly online software for calculation of parameters relevant to radiation shielding and dosimetry. **Rad. Phys. Chem.**, v. 166, p. 1-12, 2020, doi: https://doi.org/10.1016/j.radphyschem.2019.108496

[25] Hubbell, J.H., Seltzer, S.M., Tables of X-ray Mass Attenuation Coefficients and Mass Energy Absorption Coefficients from 1 keV to 20 MeV for Elements Z = 1 to 92 and 48 Additional Substances of Dosimetric Interest. Report NISTIR 5632, National Institute of Standards and Technology, Gaithersburg, MD 20899, 1995.

[26] Manjunatha, H. C., A study of gamma attenuation parameters in poly methyl methacrylate and Kapton. **Radiat. Phys. Chem.**, v. 137, p. 254 – 259, 2017.

[27] Devillers, M. A. C., Lifetime of electrons in metals at room-temperature. **Solid State Commun.**, v. 49, p. 1019 – 1022, 1984.

[28] Aboudeif, Y., et al., An evaluation of the radiation protection characteristics of prototyped oxide glasses utilizing PhyX/PSD software, **J. Instrum.** v. 15, n. 8, p. P08005, 2020.

[29] Shultis J. K., Faw, R. E., **Fundamentals of Nuclear Science and Engineering**, 2nd ed. CRC Press, Boca Raton, 2008.

[30] Martin, J. E., **Physics for radiation protection** (2nd ed.). Weinheim: Wiley-VCH Verlag GmbH & Co. KGaA, 2006.

LICENSE